Effects of substrate temperature on nanostructure and band structure of sputtered Co3O4 thin films

AUTHOR(S):

Yamamoto, Hiroki; Tanaka, Shuhei; Hirao, Kazuyuki

CITATION:

Yamamoto, Hiroki ...[et al]. Effects of substrate temperature on nanostructure and band structure of sputtered Co3O4 thin films. JOURNAL OF APPLIED PHYSICS 2003, 93(7): 4158-4162

ISSUE DATE:

2003-04-01

URL:

http://hdl.handle.net/2433/39705

Effects of substrate temperature on nanostructure and band structure of sputtered Co_3O_4 thin films

Hiroki Yamamoto[a] and Shuhei Tanaka
Nanotechnology Glass Project, New Glass Forum, Tsukuba Research Laboratory, Tsukuba Research Consortium, 9-9, 5-Chome, Tokodai, Tsukuba, Ibaraki, 300-2635, Japan

Kazuyuki Hirao
Division of Material Chemistry, Graduate School of Engineering, Kyoto University, Yoshida-honmachi, Sakyou-ku, Kyoto, 606-8501, Japan

(Received 5 August 2002; accepted 3 January 2003)

Effects of substrate temperature (T_s) on nanostructure and band structure of sputtered Co_3O_4 thin films were investigated. The lattice constant of Co_3O_4 sputtered at room temperature was longer than the reported bulk Co_3O_4 value. It decreased with increasing T_s and approached the reported value. Average grain size of the film formed at $T_s=918$ K was 13.6 nm which was twice as big as that of the film obtained at $T_s=293$ K. Intensities of optical absorption peaks increased with increasing T_s. Band gaps corresponding to the charge transfer from $Co^{2+}(\pi^*e)$ to $Co^{2+}(\pi^*t_2)(0.8\,\text{eV})$, from $Co^{3+}(\pi^2t_2)$ to $Co^{2+}(\sigma^*t_2)(1.3\,\text{eV})$, and from $O^{2-}(\pi^*\Gamma)$ to $Co^{2+}(\sigma^*t_2)\,(2.1\,\text{eV})$ increased as a function of T_s. Detailed analysis of the optical absorption spectra in the infrared region indicated that there were many kinds of defects in the Co_3O_4 thin film formed at $T_s=293$ K and there were fewer defects in the film formed at $T_s=918$ K. The defects, low density, and increasing interface area at intergrains of nanoparticles caused a lowering of E_g at lower substrate temperature. © *2003 American Institute of Physics.* [DOI: 10.1063/1.1555681]

I. INTRODUCTION

Co_3O_4 thin films have significant optical nonlinearity which is derived from their nanostructure and band structure.[1–8] To obtain Co_3O_4 thin films, the sol-gel,[9] chemical vapor deposition,[10] spray pyrolysis,[11] and sputtering[12] methods are used. The sputtering method is useful because it is applicable to optical disks, magnetic disks, and other electronic and optical devices.[5,13] However, it imparts a high energy to the source materials, and as they are quenched on the substrate, the thin film obtained is in a nonequilibrium state. Transition metal oxides like Co_3O_4 easily change their valence states, so many kinds of defects will exist in their sputtered thin films.

One of the effective parameters that improves the structure of thin films is substrate temperature (T_s) during sputtering because it changes the quenching conditions of the source materials. In the present study, we focus on the effects of T_s on the optical properties, defects, nanostructure, and band structure of Co_3O_4 thin films, and we discuss the relationship among these parameters.

II. EXPERIMENTAL PROCEDURE

The Co_3O_4 films were obtained by rf magnetron sputtering on silica glass substrates. An SPF-750HL sputtering device (Anelva Techno Business Co. Ltd.) was used to form the thin films. The substrate temperature was changed from 293 to 918 K. 99.9999% argon gas was used as sputtering gas. Sputtering power was 1.0 kW on a 152.4 mm ϕ Co_3O_4 target. Each film had about 70 nm thickness. Back pressure was under 4.0×10^{-5} Pa, and the pressure during sputtering was 7.0×10^{-1} Pa.

The lattice constant, a axis of the normal spinel structure of Co_3O_4, was measured using wide range x-ray diffraction (XRD, Rigaku RU-200). The nanostructure was evaluated by transmission electron microscopy (TEM), and a Hitachi H-9000NAR was used for those observations. The acceleration voltage was 300 kV. The specimens for TEM were prepared with an ion milling device (Gatan Model 600 N).

Optical absorption spectra of the films were measured by an optical spectrum analyzer (Hitachi Ltd., U-3500). They were calculated from transmittance and reflectance spectra. Transmittance and reflectance of the substrate were subtracted as the baseline. The detailed structure of the optical absorption spectra in the infrared region was measured using an optical spectrum analyzer (Ando Electric Co. Ltd., AQ-6315A) with white light (Ando Electric Co. Ltd., AQ-4303B).

III. RESULTS

A. Lattice constant and nanostructure of Co_3O_4 thin films

Figure 1 shows the lattice constant (a axis) of Co_3O_4 thin films calculated from the XRD pattern of the thin films as a function of the substrate temperature in the sputtering process (T_s). The lattice constant decreased with increasing T_s. According to powder diffraction results, the lattice constant of Co_3O_4 was 0.808 nm.[9] Therefore the lattice constant of Co_3O_4 film formed at lower T_s was larger, and it approached the reported value as T_s was increased.

[a]Electronic mail: h-yama@ngp.trc-net.co.jp

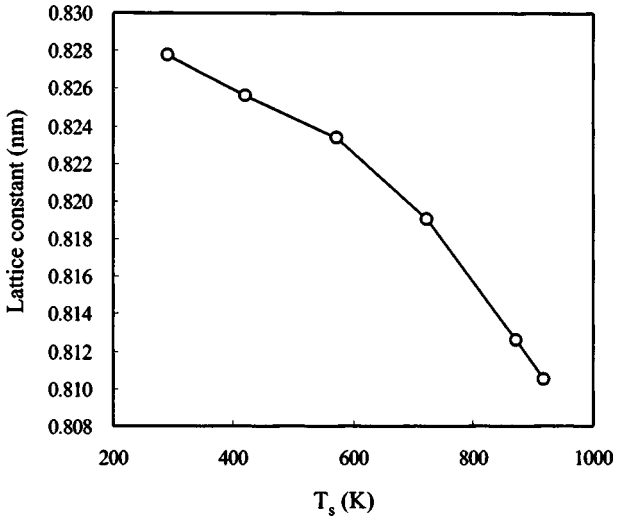

FIG. 1. Lattice constant of Co_3O_4 thin films as a function of substrate temperatures (T_s).

Figure 2 shows the intensity of peaks 111, 311, and 511 and their summation as a function of T_s. From 273 to 593 K, there were no significant changes in the intensity of the peaks. Peak 111 increased dramatically in the T_s region from 723 to 918 K. Peaks 311 and 511 increased from 723 to 873 K. The summation of the intensity of these peaks also increased, indicating the improved crystallinity or grain growth obtained by increasing T_s.

In the lower T_s region under 423 K, peak 311 was dominant indicating that the Co_3O_4 thin films had a random orientation because peak 311 is the highest in the powder diffraction pattern of Co_3O_4.[9] On the other hand, peak 111 was the highest in higher T_s regions above 573 K, showing that the Co_3O_4 films had a 111 orientation tendency.

Figure 3 shows the high resolution TEM image of the Co_3O_4 thin films formed at (a) $T_s = 293$ K and (b) 918 K. Both films consisted of nanoscale particles, and the lattice image indicated that these particles were Co_3O_4. The grain size of Co_3O_4 thin films obtained at 918 K of T_s was almost twice as big as that of the films obtained at 293 K. A grain boundary phase, 1.0 nm thick, could be observed in both films.

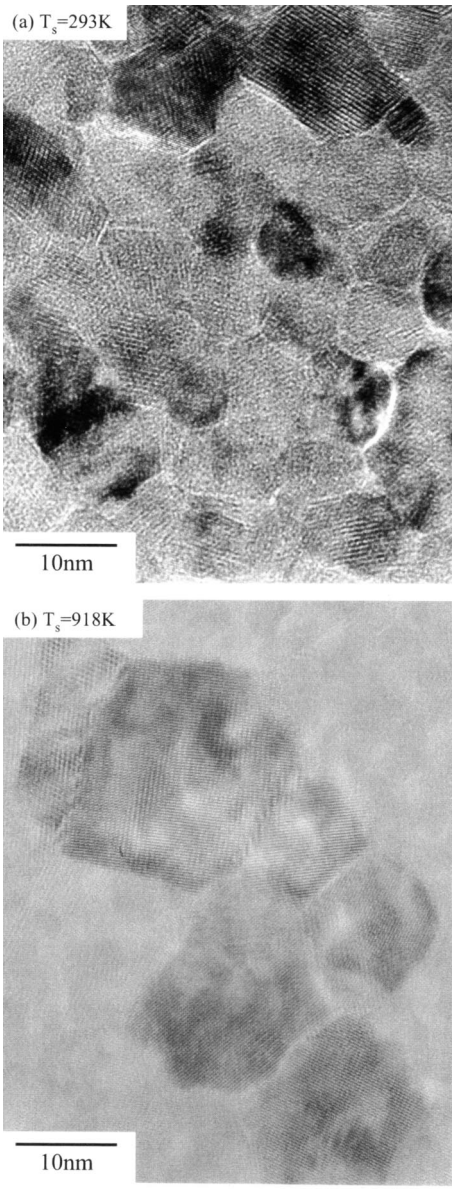

FIG. 3. Transmittance electron micrographs of the Co_3O_4 thin films obtained at T_s of (a) 293 K and (b) 918 K.

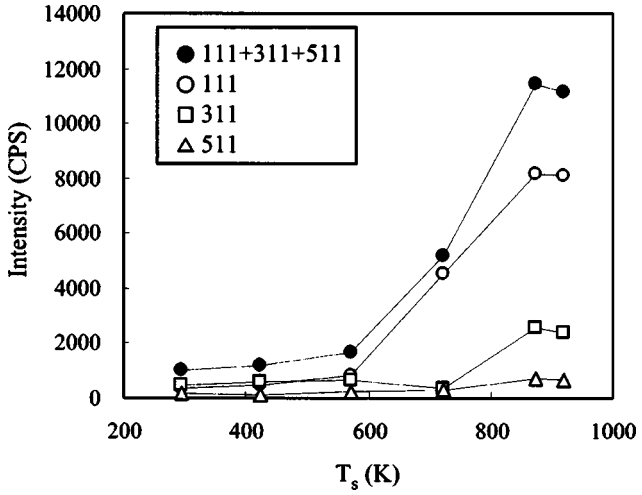

FIG. 2. Peak intensities of x-ray diffraction patterns of Co_3O_4 thin films obtained at several substrate temperatures.

To investigate the grain size in detail, we calculated the grain size dispersion. Figure 4 shows the dispersion of the grain size of the Co_3O_4 thin films obtained at $T_s = 293$ and 918 K calculated from the film TEM images. The average grain size (d) of Co_3O_4 thin film formed at 293 K was 7.40 nm and the standard deviation of the grain size (σ) was 1.69 nm. The d and σ of Co_3O_4 film formed at 918 K were 13.6 and 3.63 nm, respectively. Therefore d and σ of Co_3O_4 film formed at 918 K were almost twice and eight times, respectively, as big as those of the Co_3O_4 thin film formed at 293 K. The grain growth at higher substrate temperatures is one cause of the increased total intensity of the XRD pattern seen in Fig. 2.

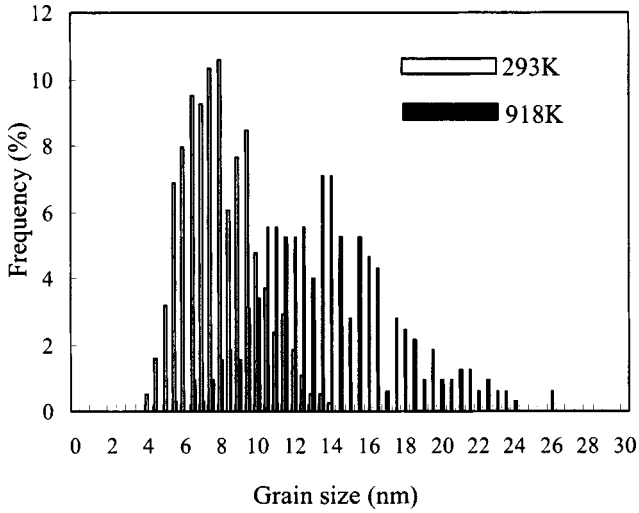

FIG. 4. Grain size dispersion of the Co_3O_4 thin films formed at T_s of 293 and 918 K.

B. Optical absorption spectra and band gap energy estimation

Figure 5 shows the optical absorption spectra of Co_3O_4 thin films formed at several substrate temperatures. Co_3O_4 films had some absorption peaks at 0.75, 0.9, 1.7, and 3.0 eV. The intensities of all absorption peaks increased with increasing T_s. Figure 6 shows the detailed optical absorption spectra of the Co_3O_4 thin films obtained at $T_s=293$ and 918 K in the wavelength region from 0.75 to 1.25 eV. A lot of small absorption peaks were observed in the spectrum of the sample formed at $T_s=293$ K. Such small absorption peaks, which looked like the noise signals of the thin films formed at room temperature, were reproducible. The small peaks in the near infrared region were due to defects including interface area at intergrains of nano particles in the Co_3O_4 crystals. On the other hand, there was a broad peak corresponding to 0.75 and 0.9 eV of absorption peaks in the spectrum of the sample obtained at $T_s=918$ K instead of the small absorption peaks. Therefore the defects in the film formed at higher T_s were fewer in number than for the film formed at lower T_s, and absorption peaks due to the Co_3O_4 structure that was defect-free appeared in the sample formed at higher T_s.

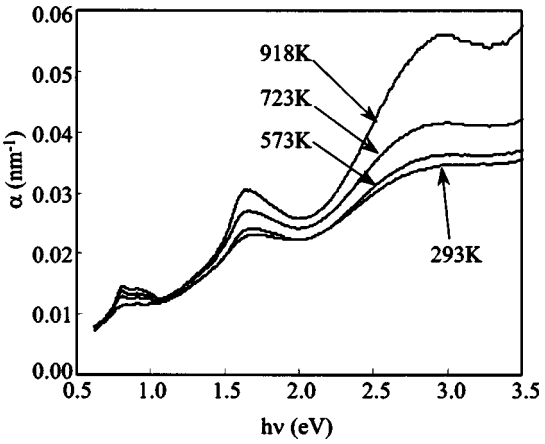

FIG. 5. Optical absorption spectra of Co_3O_4 thin films formed at T_s of 293, 573, 723, and 918 K.

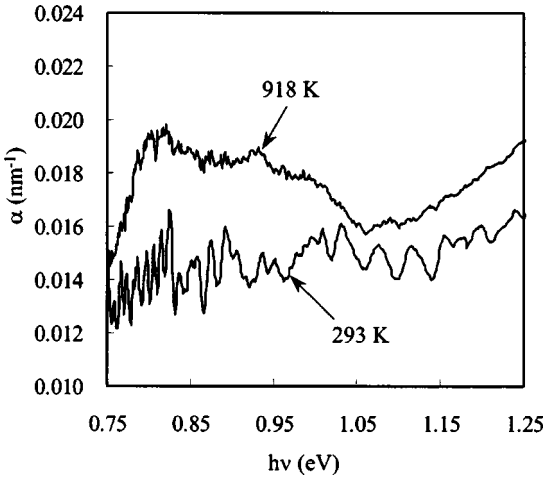

FIG. 6. Detailed measurements of the optical absorption spectra of the Co_3O_4 thin films obtained at 293 K and 918 K in the near infrared region.

To investigate the details of the band structure of these films, we estimated the allowed direct transition energy using the formula[11]

$$\alpha=\alpha_0\frac{(h\nu-E_g)^n}{h\nu}. \tag{1}$$

Here α is an absorption coefficient, α_0 is a constant, and $h\nu$ is the photon energy. In the allowed direct transition, $n=\frac{1}{2}$. Hence

$$(ah\nu)^2=\alpha_0^2(h\nu-E_g), \tag{2}$$

if

$$\alpha h\nu\rightarrow 0, \quad h\nu=E_g.$$

Therefore extrapolation of the straight line portion to zero absorption coefficient in the $(\alpha h\nu)^2$ versus $h\nu$ curves gives band gap energy E_g.

Figure 7 plots $(\alpha h\nu)^2$ versus photon energy. Patil *et al.*[11] showed that there are two energy levels of the direct allowed transition at 2.0 and 1.3 eV in the Co_3O_4 thin films. We found that other band gaps were present at lower photon energies, about 0.7 and 1.0 eV. These two peaks were overlapped, so we could not decide an accurate value for the band gap of 1.0 eV, although we found E_g of 0.7 eV. The slope of the tangential line for each band gap was less, and the band gaps shifted to lower energy with increasing substrate temperature.

It has been reported that Co_3O_4 has band gaps at 0.8, 1.0, 1.3, and 2.1 eV, and E_g at 0.8, 1.3, and 2.1 eV are assigned as charge transfers from $Co^{2+}(\pi^*e)$ to $Co^{2+}(\pi^*t_2)$, from $Co^{3+}(\pi^2t_2)$ to $Co^{2+}(\sigma^*t_2)$, and from $O^{2-}(\pi^*\Gamma)$ to $Co^{2+}(\sigma^*t_2)$, respectively.[14–17] We considered that the reported 0.8 eV corresponded to the 0.7 eV value observed in the present study. The calculated E_g's around 0.7, 1.3, and 2.1 eV, which could be given accurately from Fig. 7, are plotted as a function of T_s in Fig. 8. Every E_g value increased as a function of T_s.

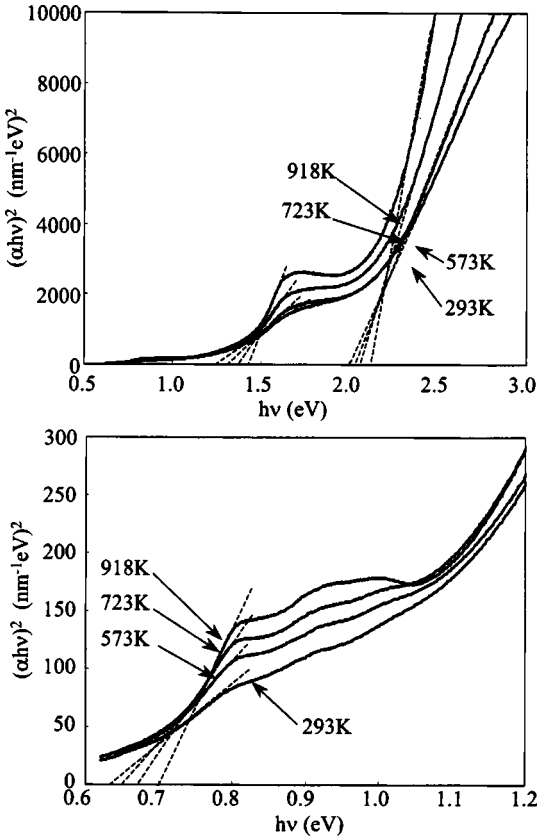

FIG. 7. $(\alpha h\nu)^2$ vs photon energy $(h\nu)$ for several substrate temperatures (T_s).

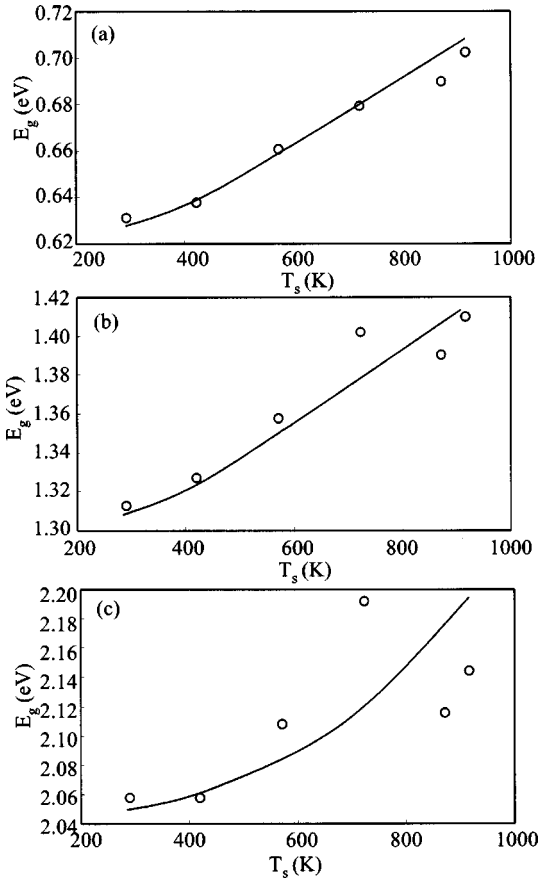

FIG. 8. Band gap shift of Co_3O_4 thin films as a function of substrate temperatures (T_s), (a) $E_g = 1.30$ eV and (b) $E_g = 2.06$ eV.

IV. DISCUSSION

In this section, we consider the relation among the nanostructure, defects, and band structure of the sputtered Co_3O_4 thin films and discuss the effects of the substrate temperature on them.

The lattice constant of the Co_3O_4 films obtained at lower T_s is large, and it approaches the reported value with increasing T_s. This indicates that densification of the Co_3O_4 films progresses with increasing T_s. Peak intensities of XRD and TEM images show that a higher T_s leads to larger grain size of the Co_3O_4 particles, and the grain size of the Co_3O_4 film formed at 918 K of T_s is almost twice as big as that of the film formed at 293 K of T_s. The total XRD peak intensity of the film formed at $T_s = 918$ K is ten times as large as that formed at 293 K of T_s, which is caused by the densification and grain growth of the Co_3O_4 films on increasing T_s. The grain growth causes the interface area at intergrains to decrease. Figure 6 indicates that many kinds of defects exist in the Co_3O_4 film formed at 293 K, and the one formed at 918 K has fewer defects. Therefore increasing T_s causes densification, grain growth, and fewer defects of the Co_3O_4 thin films.

According to E_g analysis, a blueshift of the band gap is observed with increasing T_s. To consider the relationship between the structure of Co_3O_4 films and band gap energy E_g we consider the band structure of the Co_3O_4 films at high and low substrate temperatures. Figure 9 shows a schematic diagram of the energy bands of Co_3O_4 formed at (a) 918 K and (b) 273 K of T_s. The film obtained at $T_s = 918$ K has fewer defects, a smaller interface at intergrains because of grain growth, and dense crystals like bulk Co_3O_4, so that the energy level of the bands has high uniformity in all the films. Therefore, E_g is close to constant, and the absorption peak is consequently higher and sharper. On the other hand, as shown in Fig. 9(b), the bands in the Co_3O_4 thin films have many defects, a lot of interfaces, and a lower density, so that there are many defects and interface levels and splitting of the bands into several energy levels occurs. Therefore many kinds of transition conditions near the band gap energy oc-

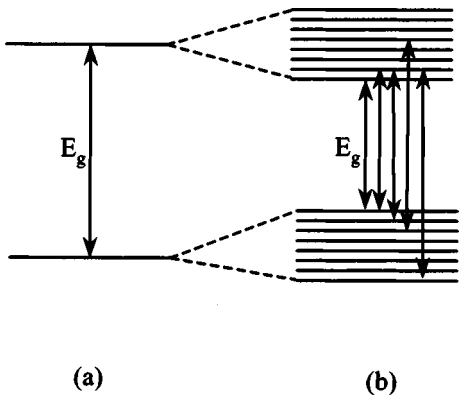

FIG. 9. Schematic diagram of the band structure of Co_3O_4 thin films obtained at (a) 918 K and (b) 273 K.

cur. Simultaneously, the redshift of the minimum band gap energy is also observed. Consequently the broadening and the redshift of the band gap energy observed in the thin films are formed at lower T_s.

Next, we discuss the effects of T_s on the structure of Co_3O_4 thin films thermodynamically. In the sputtering process, the migration speed of the source materials on the substrate determines the structure of the thin films. At high substrate temperatures (918 K in the case of Co_3O_4), the migration speed of the atoms or ions is fast because they have high energies on the hot substrate. Therefore the grain growth speed is higher than the nucleation speed and the grain growth is dominant at high temperatures. Consequently, the grain size of the film formed at 918 K is bigger than that of the film formed at 273 K. The source materials have efficient energy to migrate, so epitaxial grain growth occurs easily. Therefore fewer defects occur in the film obtained at high temperatures.

At high substrate temperatures, it is also easy to overcome the energy barrier to form the 111 orientation of the spinel structure, in which the close-packed surface of the oxygen atoms faces parallel to the substrate surface. Therefore the 111 orientation found at high temperatures is as shown in Fig. 2. However, the relation between the orientation and the blueshift of the band gap energy of Co_3O_4 thin films is not clear from this study.

V. CONCLUSIONS

We obtained the following results on the effects of substrate temperature (T_s) in the sputtering process on nanostructure and band structure of Co_3O_4 thin films. According to our investigation on the lattice constant of sputtered Co_3O_4 thin films, the densification progressed at high substrate temperatures, and it approached the reported value of the bulk Co_3O_4. Also, TEM observations indicated that grain growth occurred simultaneously. Optical absorption spectra showed that defects in the Co_3O_4 thin film decreased at high substrate temperatures. Band gaps corresponding to the charge transfer from $Co^{2+}(\pi^*e)$ to $Co^{2+}(\pi^*t_2)(0.8\,\mathrm{eV})$, from $Co^{3+}(\pi^2t_2)$ to $Co^{2+}(\sigma^*t_2)(1.3\,\mathrm{eV})$, and from $O^{2-}(\pi^*\Gamma)$ to $Co^{2+}(\sigma^*t_2)(2.1\,\mathrm{eV})$ increased with increasing T_s. The defects, low density, and increasing interface area at intergrains of nanoparticles caused a lowering of E_g at low substrate temperatures.

ACKNOWLEDGMENT

This work was carried out in the Nanotechnology Glass Project as part of the Nanotechnology Materials Program supported by the New Energy and Industrial Technology Development Organization (NEDO).

[1] M. Ando, K. Kadono, M. Haruta, T. Sakaguchi, and M. Miya, Nature (London) **374**, 625 (1995).
[2] T. Shintani, K. Moritani, A. Hirotsune, M. Terao, H. Yamamoto, and T. Naito, Joint MORIS/ISOM '97 Post-deadline Papers Technical Digest (1997), p. 23.
[3] T. Shintani and M. Terao, Opt. Alliance **9**, 10 (1998) (in Japanese).
[4] H. Yamamoto, T. Naito, M. Terao, and T. Shintani, Digest of 11th Fall Meeting of Ceramic Society of Japan (1998), p. 243.
[5] T. Shintani, M. Terao, H. Yamamoto, and T. Naito, Jpn. J. Appl. Phys., Part 1 **38**, 1656 (1999).
[6] H. Yamamoto, T. Naito, and K. Hirao, Mater. Res. Soc. Symp. Proc. **703**, V13.20.1 (2002).
[7] H. Yamamoto, T. Naito, M. Terao, and T. Shintani, Thin Solid Films **411**, 289 (2002).
[8] H. Yamamoto, S. Tanaka, T. Naito, and K. Hirao, Appl. Phys. Lett. **81**, 999 (2002).
[9] F. Svegl, B. Orel, M. G. Hutchins, and K. Kalcher, J. Electrochem. Soc. **143**, 1532 (1996).
[10] T. Maruyama and S. Arai, J. Electrochem. Soc. **143**, 1383 (1996).
[11] P. S. Patil, L. D. Kadam, and C. D. Lokhande, Thin Solid Films **272**, 29 (1996).
[12] W. Estrada, M. C. A. Fantini, S. C. de Castro, C. N. Polo da Fonseca, and A. Gorenstein, J. Appl. Phys. **74**, 5835 (1993).
[13] X. Song, J. Sivertsen, and J. Judy, J. Appl. Phys. **81**, 4387 (1997).
[14] J. G. Cook, M. P. van der Meer, and D. Hogg, J. Vac. Sci. Technol. A **4**, 607 (1986).
[15] J. G. Cook and M. P. van der Meer, Thin Solid Films **144**, 165 (1986).
[16] K. M. E. Miedzinska, B. R. Hollebone, and J. G. Cook, J. Phys. Chem. Solids **48**, 649 (1987).
[17] M. Lenglet and C. K. Jorgensen, Chem. Phys. Lett. **229**, 616 (1994).